

Development of Energy- and Angle-Resolving Analyzer for Surface Electron Spectroscopic Tomography

Shingo Ichimura¹⁾ and Akira Kurokawa

*Electrotechnical Laboratory
1-1-4, Umezono, Tsukuba 305, Japan
E-mail: shingo@etl.go.jp¹⁾*

(Received: Jan. 30, 1997 Accepted: Feb. 21, 1997)

Abstract

The design and characteristics of the energy- and angle resolving analyzer, which is constructed aiming at the development of the surface electron spectroscopic tomography (SET) technique, is described together with the whole experimental system. The analyzer has a wide detection angle of π steradian, and the energy resolution of about 1% ($\Delta E/E$ value) which could be obtained by the attachment of two retarding grids fabricated by a unique method. The analyzer allowed angular- and energy-resolved imaging of Si LVV Auger signals within acceptable time (typically; 100 sec.) with primary beam of 10 kV and 10 nA. In the angular- and energy-resolved image for the reconstructed Si(111)7 \times 7 surface, enhancement of the Auger signal intensity along the direction of [110] was observed, reflecting the row of nearest neighbor atoms in surface few layers.

1. Introduction

Recent development of sophisticated film formation techniques such as molecular beam epitaxy (MBE) and/or metal-organic chemical vapor deposition (MOCVD) techniques allows precise control of composition and structure of ultrathin layers. In the case of GaAs/AlAs super lattice, for example, the thickness of each layer is now in the range of a few nanometer (nm). So the formation of an ideal interface having the abruptness of one atomic layer between two different materials becomes real target. It is also true for silicon technology, since the continuous scaling down of semiconductor device dimensions requires the formation of ultrathin silicon oxide film (with the thickness of a few nm) on silicon substrate.

The abruptness of the interface structure between the two different materials is often investigated by cross sectional observation with transmission electron microscope (TEM), and photographs showing almost one atomic layer roughness at the interface is often presented especially for semiconductor super lattice [1]. It should be reminded, however, that the TEM observation gives only the structural information averaged along the interface layers, and it is not so sensitive to local roughness change. Other techniques which is often applied for the analysis of surface layer composition and/or structure are AES (Auger electron spectroscopy) and XPS (X-ray photoelectron spectroscopy). These surface sensitive techniques must be combined with ion

sputtering to perform in depth analysis. So they cannot avoid the problems arising from the sputtering such as interface mixing and roughness formation, in addition to their inherent problem that the signals (Auger- and photo-electron signals) are averaged within escape depth (inelastic mean free path; IMFP) of those electrons. Therefore, a new method which can get rid of the problems associated with conventional surface characterization techniques has also to be persuaded to establish precise film formation techniques with one atomic layer controllability.

The idea of surface electron spectroscopic tomography (SET) technique is proposed as a new characterization method which is non-destructive and allows to identify atomic species and atomic arrangement in the first few atomic layers with layer by layer resolution [2]. It bases on the precise analysis of angular modifications of Auger (photo) electron intensities not only at the peak position but also at the tail position of the peak to extract the cross sectional view, since the modification reflects elastic and/or inelastic scattering which Auger (photo) electrons have suffered before they escape from the surface. Although surface structure analysis have been reported in holographic manner with the observation of elastically scattered electrons in angle-resolved detection [3], the angle-resolved detection of inelastically scattered electrons was not performed so far, mainly because the acquisition of Auger (photo) electron peak

and its loss tails for every ejection angle needs long experimental time.

The aim of the present paper is to report fundamental characteristics of angle- and energy-resolving analyzer, which is constructed as the first step for the development of SET technique.

2. Construction of the Experimental Apparatus

Fig.1 (a) and (b) shows the scheme of the experimental setup. The vacuum chamber is made of stainless steel 316L which was electrolytically polished and was pre-baked at about 723 K for 72 hours under ultrahigh vacuum condition (about 10^{-7} Pa). This pretreatment is essential to reduce out gassing from the chamber wall and to get extremely high vacuum (XHV) condition [4]. A magnetic (μ -metal) shield is placed in the XHV chamber, and the total system is then evacuated to 10^{-9} Pa by two turbo molecular pumps (1500 l/s and 150 l/s) which are connected in series.

The chamber is equipped with the angle- and energy-resolving analyzer which will be described in detail below, a Knudsen cell (K-cell) and an electron beam gun (e-gun) for molecular beam supply, and an electron beam system which is originally used for micro probe Auger equipment [JEOL; 7100E]. Electron

beam is chosen as a primary source since it give possibility of local area analysis. The vacuum chamber is also equipped with an ozone jet generator, which supplies high purity (>80 at.%) and high flux ($>10^{16}$ molecules/s) ozone molecules [5], to form finely controlled thin SiO₂ film on Si substrate at room temperature [6]. It is now used to establish the layer by layer formation process and is planed to be "in-situ" monitored by the SET technique.

Fig.2 shows the schematic view of the energy- and angle resolving energy analyzer. It is based on simultaneous angle resolved electron energy spectrometer [Shimazu; SAREES] which consists of two large sphere grids. The analyzer has a wide detection angle (π steradian), and electrons ejected in this solid angle are energy selected by the potential V 's supplied to the outer sphere grid. In addition, the ejection angle of each electron is conserved when it passes the exit aperture of the analyzer. Then, the angular distribution of electrons having a selected energy is converted to bright spot distribution on a fluorescent screen which is placed after a micro channel plate intensifier (MCP). The MCP has the size of 105 mm in diameter, and the gain of about 10^6 . The image on the fluorescent screen is taken with a CCD (charge-coupled device) camera, which has 512×512

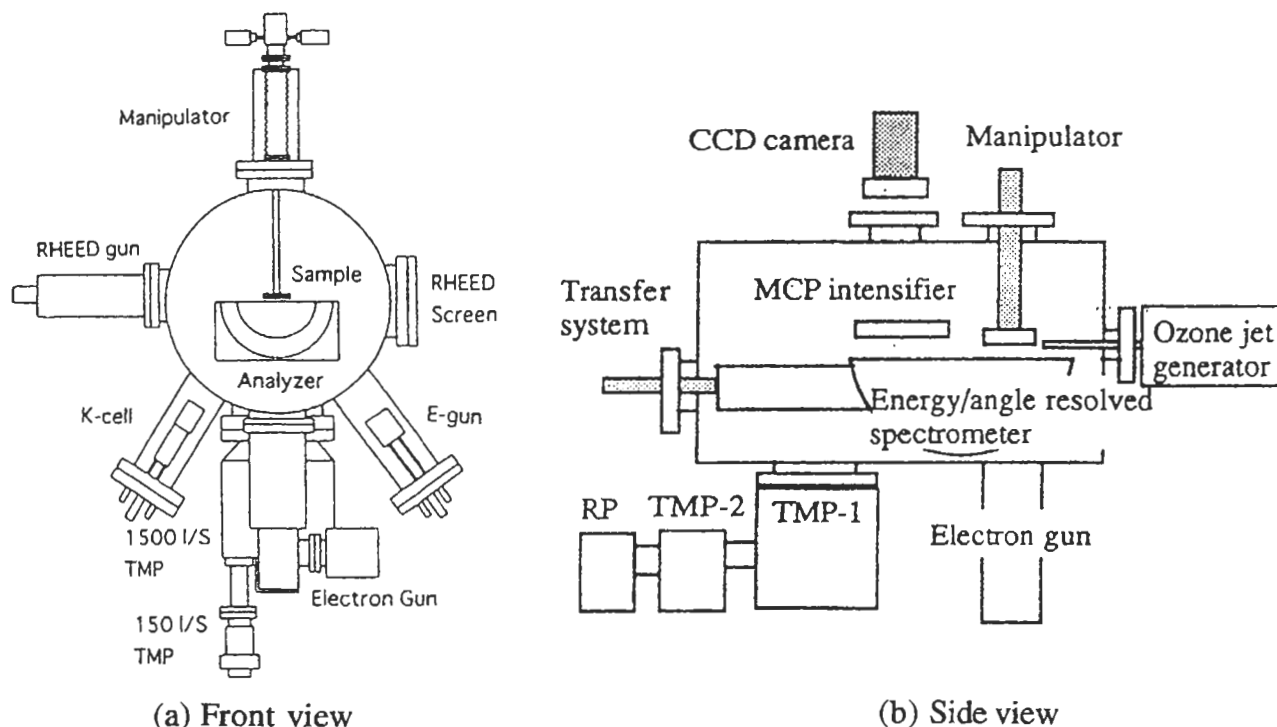


Fig. 1 Schematic front view (a) and side view (b) of the scheme of the experimental setup for surface electron spectroscopic tomography.

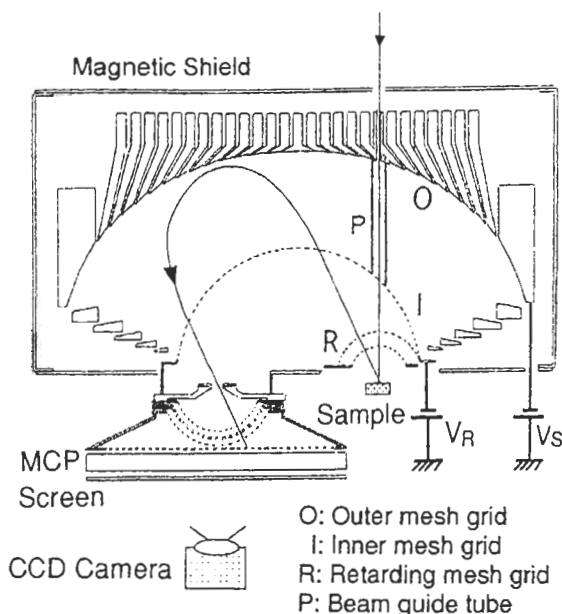


Fig. 2 Schematic view of the energy- and angle resolving energy analyzer with a special retarding grids.

pixel array and is cooled down to liquid nitrogen temperature.

Since the incident beam slit and the sample position are not placed at the center of the two sphere grids, the primary beam is deflected by an electrostatic fields associated with the potential difference ($V_S - V_R$) between the two grids. To avoid the deflection, a beam guide is inserted into the analyzer so that electron passes straight [7].

3. Results and Discussion

3.1 Principle and Transmission of the energy analyzer

The characteristic response of the SAREES is analyzed and reported by Daimon [8]. The energy resolution of the analyzer obeys the following equation;

$$\Delta n = \frac{2m^2 \cos \beta}{\sqrt{\alpha^2 - m^2 \sin^2 \beta}} \frac{\Delta E}{E} + \frac{2m^3 \sin^2 \beta}{\alpha^2 - m^2 \sin^2 \beta} \left(\frac{\Delta E}{E} \right)^2 \quad (1)$$

Here, as is shown in Fig.3 (a), α is the ejection angle of electron (with energy E) from the point P_1 (sample position; the distance from the center is m) and β is the incidence angle of the electron to the point P_2 (aperture position; the distance n). In the present system, $m=n=42$ mm and $\alpha=\beta$. For an electron ejected from the same point P_1 with the same ejection angle but with a different energy of $E+\Delta E$, it cross the x-axis at another point. Δn indicates the distance between the point and P_2 . It is clear from eq.(1)

that the energy resolution of the analyzer is not constant but depends on the ejection angle of electrons. The energy resolution decreases at larger ejection angles (i.e., at around $\alpha=\pi/2$). We have calculated the transmission of the analyzer assuming several ejection points (i.e., incident point of the primary electron beam) along x and y direction. The results are shown in Fig. 3(b) for the shift of ejection point in x-direction, and in Fig.3(c) for the shift in y direction. The horizontal axis in Fig.3 indicate the ratio of electron energy (E) and the fixed pass energy ($E_s=eV_s$; e is a unit charge). Here, the size of the exit aperture is 1 mm, and the inner sphere grid is assumed to be grounded (i.e., $V_R=0$; see Fig.2). It is clear in Fig.3(b) that the analyzer has a specular transmission function for the shift of ejection point in the x-direction; not electrons having a selected energy E_s but those having larger or smaller energy than E_s come to mainly pass the analyzer. This suggests the importance of adjusting and fixing the incident point of primary electron beam, which could be achieved by the insertion of the electron beam guide mentioned above. For the shift of primary beam position in y-direction, the shape of the transmission function does not change so much, although it results in decreasing of the

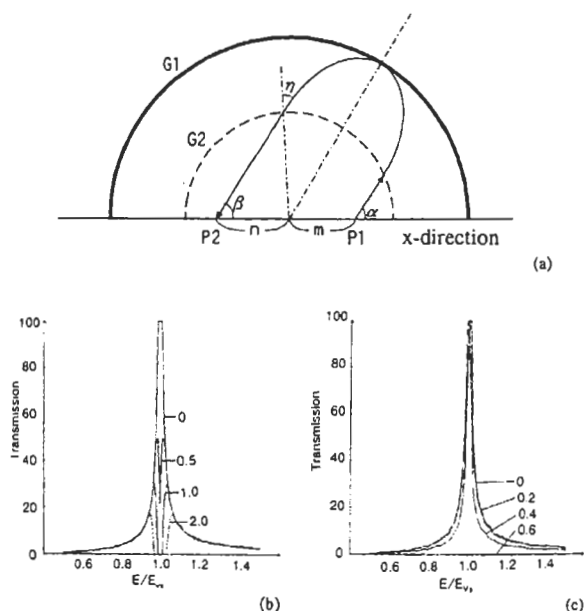


Fig. 3 Illustration of electron trajectory in the angle- and energy resolving analyzer (a), and calculated transmission characteristics of the analyzer for several ejection points along x direction (b) and direction (y). The horizontal axis in (b) and (c) indicate the ratio of electron energy (E) and the fixed pass energy.

transmission as is seen in Fig. 3(c).

3.2 Improvement of the energy resolution of the analyzer

The original energy resolution of the analyzer (SAREES) was only about 5% ($\Delta E/E$ values), mainly due to the reduction of energy resolution near surface normal direction (see eq.(1)). This resolution is too poor to analyze the loss structure of an Auger peak. We have tried to improve the energy resolution by setting two retarding grids (spherical shape) between the sample and the sphere grids of the analyzer. The radius of the inner grid is 15 mm, and that of outer grid is 22 mm. The inner grid was biased to ground potential, and the outer grid was biased at the same potential with the inner sphere grid. Thus, the constant pass energy analysis is possible by sweeping the bias of inner spherical grid (V_R) keeping the pass energy (i.e., $V_s - V_R$) at constant. The inserted retarding grids is also described in Fig.2. The angular distribution of ejected electrons must not be affected by the insertion of the

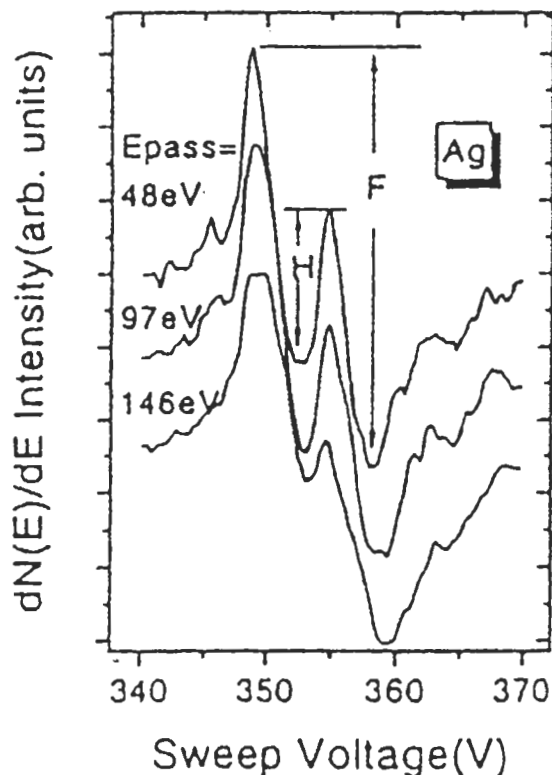


Fig. 4 Ag Auger spectrum taken with constant pass energy of 48 eV, 97 eV, and 146 eV. The primary electron beam and current was 10 keV and 10 nA, and the acquisition time was 1 min. $N(E)$ spectra was numerically differentiated to estimate the ratio of H/F.

retarding grids. In order to satisfy this requirement, we have constructed a special pair of spherical grids, each of which have 3,800 drilled holes and the diameter of each hole is 0.73 mm for outer grid and 0.5 mm for inner grid, and the grids was placed so that the both holes cover the same solid angle to the incident point of the primary beam [9].

Fig.4 shows Ag Auger spectrum taken with constant pass energy of 48 eV, 97 eV, and 146 eV. The primary electron beam and current was 10 keV and 10 nA, and the acquisition time was 1 min. $N(E)$ spectra was numerically differentiated to estimate the ratio of H/F (for the definition of H and F, see Fig.4), since it is reported that the ratio gives good indication of the analyzer energy resolution[10]. We have confirmed that the energy resolution was improved to 1.0, 1.1, and 1.2 % ($\Delta E/E$ values) for pass energy of 48, 97, and 146 eV, respectively.

3.3 Measurement of angular dependency of Auger signal intensity

Fig.5 shows a Si Auger spectra taken with Si(111) sample, which was thermally flashed to 1473 K before the measurement. No carbon and oxygen peak appeared on the spectrum, and it was expected that the surface was reconstructed to 7×7 structure since we had observed 7×7 LEED pattern for a Si(111) sample treated with the same procedure. The primary beam current in the experiment is 10 nA with the primary energy of 10 kV, and the time for the measurement is 100 sec. The measured Si LVV peak shape and the peak to background ratio seems to be compatible with that reported in an Auger spectra handbook[11].

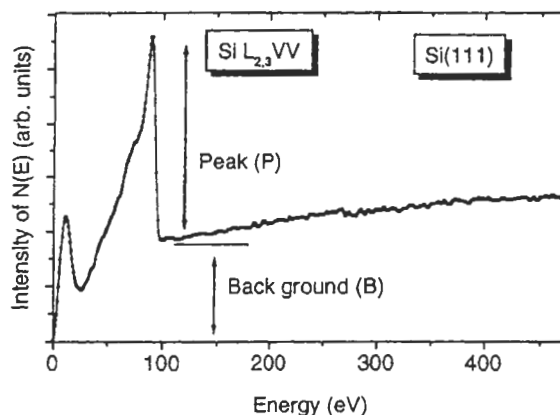


Fig. 5 Si Auger spectra taken with the primary beam current of 10 nA and the primary energy of 10 kV. The acquisition time was 100 sec.

Then, under the same primary beam condition, angular dependence of the LVV Auger signal intensity was measured. The result is shown in Fig.6. This image shows equi-intensity profile of Si LVV Auger spectrum which is obtained as follows; at first, two images were taken at the pass energy corresponding to Auger peak position (90 eV) and its background position (97 eV). Each image was taken with exposure time of 100 sec. Hereafter, the intensity profile of the images are designated as I_{90} and I_{97} , respectively. Then a processed image corresponds to the intensity profile of $(I_{90}-I_{97})/I_{90}$ was obtained to get normalized Auger intensity distribution. This ratio method is known as P/B method in AES which can reduce topographic effect. The P/B method can also cancel the intensity homogeneity arising from the analyzer transmission function. Finally, the equi-intensity profile was obtained by classifying the angular intensity.

The result shown in Fig.6. indicates that it has three fold symmetry and the appearance of stronger intensity is observable at positions indicated by x marks. The three fold symmetry becomes more clear if we take the difference of two processed images, i.e., the difference between the image shown in Fig.6 and the other image which was obtained with the same way with Fig.6 for the same sample rotated 60

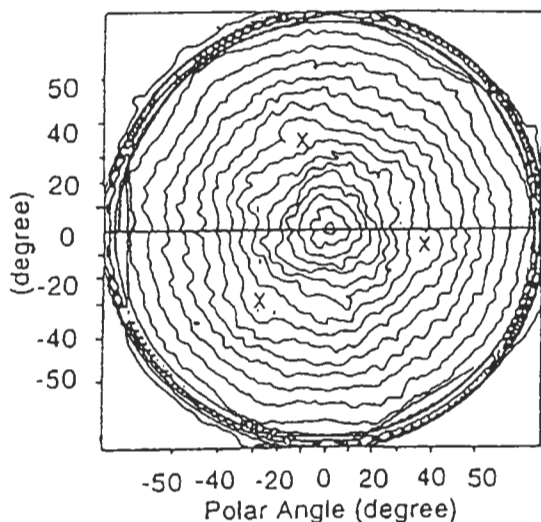


Fig. 6 The angular dependence of Si LVV Auger signal shown as an equi-intensity profile. Each line corresponds to 5% intensity step. Straight line indicates [110] direction. This image was obtained by processing Auger images taken with the primary electron beam energy and current of 10 keV and 10 nA, and the acquisition time of 100 sec.

degree around the surface normal direction as is reported elsewhere [12]. The position corresponds to [110] direction, and there is a row consisting of nearest neighbor atoms in this direction as shown schematically in Fig.7. The IMFP of Si LVV Auger electron is about 0.45 nm, which is calculated using TPP (Tanuma-Powell-Penn)-2 equation [13], and is too short to reflect the atomic arrangement in the bulk atomic structure. Therefore, the observed angular dependence of Auger signal intensity reflects atomic structure in the first few layers, suggesting the possibility of SET measurement using angular modification of Auger peak intensity and its loss tail intensity.

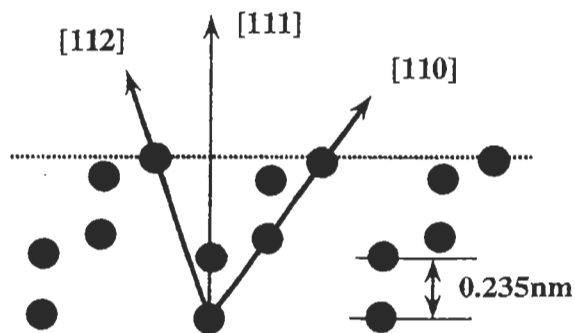


Fig. 7 Scheme for the atomic arrangement of Si(111) 7x7 reconstructed surface.

4. Conclusions

The design and characteristics of the angle- and energy-resolving analyzer is described. By the improvement in the energy resolutions of SAREES and by the attachment of the electron beam guide, it becomes possible to measure ejection angle dependence of Auger signal intensity within practical analysis time (typically, 100 sec.) with focused primary beam having a diameter of a few hundred nm. It was also confirmed that the observed Si LVV Auger image shows angular intensity distribution which is affected by the atomic arrangement in the surface few layers, suggesting the possibility of SET measurement.

Acknowledgement

The concept of SET (Surface electron spectroscopic tomography) is proposed by the collaboration with Dr. K. Yoshihara of National Research Institute for Metals. The authors would like to express their sincere appreciation to him for the stimulative discussion.

References

1. K. Kajiwara and H. Kawai, *Surf. Interf. Anal.* 15, 433 (1990)
2. Research project on "Surface atomic layer control and analysis by surface electron spectroscopic tomography" organized by the special research fund of Science and Technology Agency (1992-1994), Leader; K. Yoshihara
3. J.J. Barton, *Phys. Rev. Lett.* 61, 1356 (1988)
4. S. Ichimura, K. Kokubun, H. Shimizu, and S. Sekine, *Vacuum* 47, 545 (1996)
5. S. Ichimura, S. Hosokawa, H. Nonaka and K. Arai: *J. Vac. Sci. Technol.* A9(1991) 2369
6. A. Kurokawa and S. Ichimura, *Jpn. J. Appl. Phys.* 35 (1995) L1606
7. A. Kurokawa, S. Ichimura, and K. Yoshihara, *Jpn. Pat. No.* 83203
8. H. Daimon, *Rev. Sci. Instrum.* 59, 45 (1988)
9. A. Kurokawa, S. Ichimura, and K. Yoshihara, *Jpn. Pat. No.* 196110
10. A. Tanaka and I. Kimura, *Proc. 48th JSPS 141 Meeting*, p49; T. Ohmura and R. Shimizu, *Analytical Electron Microscopy*, ed. D.C. Joy (San Francisco Press, 1987) p333
11. T. Sekine, Y. Nagasawa, M. Kudoh, Y. Sakai, A.S. Parkes, J.D. Geller, A. Mogami, and K. Hirata, *Handbook of Auger Electron Spectroscopy*, (JEOL Ltd, Tokyo, 1982)
12. A. Kurokawa, S. Ichimura, K. Yoshihara, J.-I. Jeong, and J. Toth, *Proc. 6th European Conf. on Appl. Surf. and Interf. Anal.*, Eds., H.J. Mathieu, B. Reihl, and D. Briggs (John Wiley & Sons, Chichester, 1996) pp999
13. S. Tanuma, C.J. Powell, and D.R. Penn, *Surf. Interf. Anal.* 20, 77 (1993)